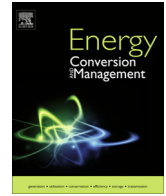


List of Publications

- [1] Zhongyuan Shi and **Tao Dong**. "Comments on "Detailed analysis for the cooling performance enhancement of a heat source under a thick plate" by Hajmohammadi MR [Energy Convers. Manage. 76 (2013) 691–700]." *Energy Conversion and Management* 129 (2016): 34-35. **Page 2**
- [2] **Tao Dong**, Zhongyuan Shi and Atle Jensen. "Bi-objective Optimization of Axial Profile of Pin Fin with Uniform Base Heat Flux." *Applied Thermal Engineering*, ATE_2017_3935_R1, under review.
- [3] **Tao Dong** and Zhongyuan Shi. "The Effect of Constant Curvature Assumption on a Evaporating Wetting Thin Film." *Heat and Mass Transfer*, HAMT-D-16-00771, under review.
- [4] **Tao Dong**, and Nuno Miguel Matos Pires. "Immunodetection of salivary biomarkers by an optical microfluidic biosensor with polyethylenimine-modified polythiophene-C 70 organic photodetectors." *Biosensors and Bioelectronics* 94 (2017): 321-327. **Page 4**
- [5] Haakon Karlsen and **Tao Dong**. "A Compact Device for Urine Collection and Transport in Porous Media." *International Conference Mechatronics*. Springer, Cham, 2017. **Page 6**
- [6] Tuan Anh Tran and **Tao Dong**. "Geometric Optimization of Complex-Shaped Cavities According to Constructal Theory ". *13th International Conference on Heat Transfer, Fluid Mechanics and Thermodynamics*, 2017. **Page 8**
- [7] Per Kristian Bolstad, Zhongyuan Shi, **Tao Dong**. "Constructal Design of Cavities for Intensified Cooling Performance on Heat Generating Volumes." *13th International Conference on Heat Transfer, Fluid Mechanics and Thermodynamics*, 2017. **Page 11**
- [8] Inventers: **Tao. Dong**, Zhongyuan Shi, Zhaochu Yang, et al. Measurement of Local Heat Transfer Coefficients of Thin Walls Based on Thermal Fluctuation Coupled Infrared Imaging, Chinese Patent Publication No.: CN 106610316 A. **Page 14**



Correspondence

Comments on “Detailed analysis for the cooling performance enhancement of a heat source under a thick plate” by Hajmohammadi M.R. [Energy Convers. Manage. 76 (2013) 691–700]



Zhongyuan Shi ^{a,b,c}, **Tao Dong** ^{d,*}

^a Institute of Applied Micro-Nano Science and Technology, Chongqing Technology and Business University, 19 Xuefu Ave., Nan'an District, Chongqing, China

^b Chongqing Engineering Laboratory for Detection, Control and Integrated System, Chongqing Technology and Business University, 19 Xuefu Ave., Nan'an District, Chongqing, China

^c Department of Mathematics, Faculty of Mathematics and Natural Sciences, University of Oslo, P.O. Box 1053, Blindern, 0316 Oslo, Norway

^d Department of Micro and Nano Systems Technology (IMST), Faculty of Technology and Maritime Sciences (TekMar), University College of Southeast Norway, Raveien 215, 3184 Borre, Norway

ARTICLE INFO

Article history:

Received 19 September 2016

Accepted 4 October 2016

Available online 7 October 2016

Keywords:

Temperature gradient spreader

Electronic cooling

Thermoeconomics

Pareto optimization

ABSTRACT

A new perspective is presented for the design practice of the temperature gradient spreader. As compared to other variables in the design space, the cooling stream velocity was found capable of rendering a better overall performance, theoretically with arbitrary adjustability. Concerning the associated pumping power consumption, the limitation from flow drag was also included in the discussion from a thermoeconomic perspective.

© 2016 Elsevier Ltd. All rights reserved.

As was indicated in [1], a trade-off exists between the minimization of the peak temperature (PT) and that of the maximum temperature gradient - MTG (originally termed as “the incremental trend of the temperature distribution”) on the bottom surface of the thick plate (hereinafter referred to as the temperature gradient spreader - TGS, since it brings about smoother temperature distribution of the heat source with a constant heat flux). The authors proposed an optimum aspect ratio (plate thickness b divided by the plate length L) for the TGS, with respect to the “balance between the imperfections through the flow system”. However, no more elaboration can be found on how this “balance” is defined, note that PT and MTG are different in physical dimensions. The investigation could have covered PT and MTG synthetically, in regard of the aspect ratio of TGS and the ratio of the longitudinal heat conduction in TGS to the convection heat transfer (the conduction-convection parameter). Moreover, other variables concerned in the design space, for instance the velocity and temperature of the inlet free stream (energy consumption associated in practice), are expected to “cooperate” with those already included for a better overall performance, from a more generic perspective.

Following the dimensional analysis [1,2], the temperature distribution at the bottom surface of TGS can be reformulated as

$$\theta(\tilde{x}, 0) = \tilde{q}\tilde{b} + 2 \sum_{n=1}^{\infty} \left(\int_0^1 \theta(\tilde{x}, \tilde{b}) \cos n\pi\tilde{x} \, d\tilde{x} \left(\frac{\cos n\pi\tilde{x}}{\cosh n\pi\tilde{b}} - 1 \right) \right), \quad (1)$$

where

$$\begin{cases} \theta(\tilde{x}, \tilde{b}) = 0.282 \left(\frac{\tilde{x}}{\kappa\tilde{b}} \right)^{-1/2} \int_0^{\tilde{x}} \left(1 - \left(\frac{\tilde{z}}{\tilde{x}} \right)^{3/4} \right)^{-2/3} \left(-\frac{\partial\theta(\tilde{z}, \tilde{y})}{\partial\tilde{y}} \Big|_{\tilde{y}=\tilde{b}} \right) d\tilde{z} \\ \tilde{b} = \frac{b}{L} \\ \kappa = \frac{2.21k_s}{k_f Re_L^{1/2} Pr^{1/3}} \end{cases} \quad (2)$$

The symbolic convention [1] is applied to all the undeclared variables and parameters in Eq. (1) and Eq. (2), note that U_{in} represents the actual velocity of the inlet free stream as compared to the counterpart (U_{∞}) of the reference case ($\tilde{b} = 0$). It is inferable that besides PT, MTG also depends on the aspect ratio \tilde{b} and the conduction-convection parameter κ , the impact from which will be discussed following the corresponding part of Section “4. Numerical Analysis” in [1]. The influence of free stream temperature at the inlet of the fluid domain is neglected in the present work since

* Corresponding author.

E-mail address: Tao.Dong@hbu.no (T. Dong).

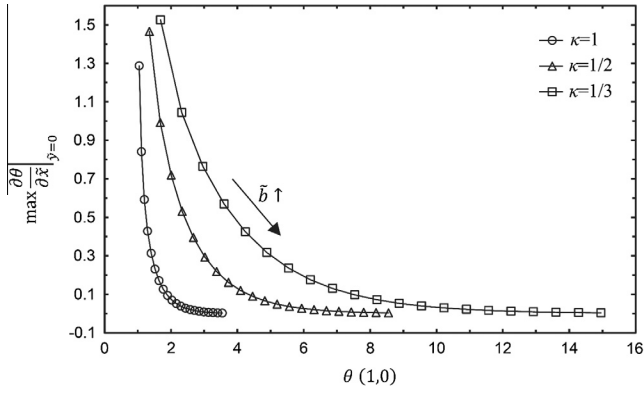


Fig. 1. The effect of the conduction-convection parameter, κ and the normalized inlet velocity of the free stream, U_{in} on the pseudo-Pareto-frontier (PPF); the aspect ratio of the TGS, \bar{b} is in the range of 0.1–2; an equal incremental step applies to any of the two adjacent points on each of the three curves consisting of 21 points in total.

- (1) the temperature is a linear term as indicated by Eq. (17) and Eq. (18) in [1], meaning that any change at the Dirichlet boundary will be transferred exactly to each inner point of the conjugated domain;
- (2) extra refrigeration may have to be included, which increases the system complexity and is not beneficial from a thermoeconomic point of view.

Fig. 1 is composed of a series of exemplary curves. Each of them depicts the trade-off between PT and MTG, with a specific κ , note that

$$\theta(1, 0) \quad (3)$$

and

$$\max \frac{\partial \theta}{\partial x} \Big|_{y=0} \quad (4)$$

stand for PT and MTG respectively in the dimensionless form. The PT increases with \bar{b} as the MTG is expectably diminished. When \bar{b} is held invariant, the difference between MTGs with different κ values also gets attenuated. Both PT and MTG are reduced in the meantime as κ decreases. In another word, a better overall performance or a Pareto dominance is achieved when the effect of laminar convection is reinforced as compared to the diffusive countercurrent of heat flow parallel to the inlet stream velocity. Further supposing that the reinforcement comes from the increased velocity of the free stream inlet U_{in} (given that the material choices for coolant fluid and TGS are limited), the concern on pumping power consumption arises since the normalized flow drag reads [3].

$$\tilde{\tau}_w = \left(\frac{U_{in}}{U_{\infty}} \right)^{3/2}. \quad (5)$$

Note that U_{∞} hereby serves as the reference velocity of the inlet free stream when $\bar{b} = 0$, Fig. 2 is indicating that the normalized flow drag has to increase super-exponentially with \bar{b} at least so

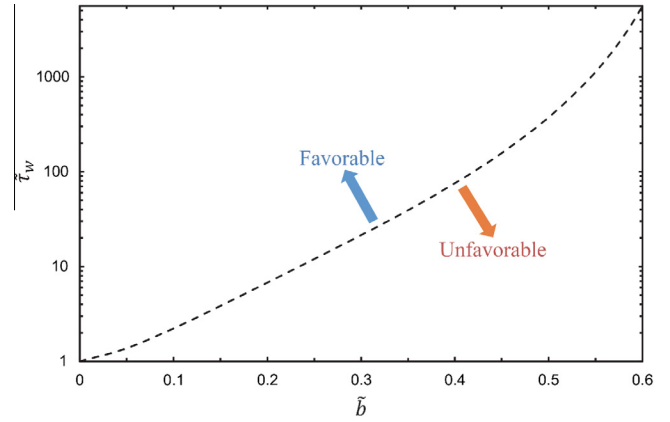


Fig. 2. The dashed curve represents the normalized flow drag $\tilde{\tau}_w$ needed for the TGS with a certain aspect ratio, so that its PT equals to that of the reference case where the TGS is absent; the region is termed as “favorable” when $\tilde{\tau}_w$ is higher than the dashed curve since the corresponding PT is lower, the opposite termed as “unfavorable”.

that the PT won’t exceed its counterpart when the cooling fluid is in direct contact with the heat source. This is a reminder that there is theoretically no optimization since the curve in Fig. 1 would ever advance toward lower PT and lower MTG simultaneously, while the better overall performance is achieved at the cost of increased flow drag, i.e. the curves are pseudo-Pareto-frontiers (PPFs). In design practice, a curb has to be identified where the cost neutralizes the benefits.

Acknowledgments

The present work, as part of the author’s (Zhongyuan Shi <zhyongyuan@uio.no> at University of Oslo) Ph.D. thesis, is supported by Trilobite Microsystems AS and Sensovann AS.

The funding support from Chongqing Research Program of Basic Research and Frontier Technology (No. cstc2015jcyjBX0004), Science and Technology Research Program of Chongqing Education Commission (No. KJ1600602), Forskningsrådet Nærings-Ph.D. (Project No.: 251129), Regionale forskningsfond Oslofjordfondet (Project Nos.: 258902 and 255893) and NANO2021 (Project No.: 263783) is hereby acknowledged.

References

- [1] Hajmohammadi MR, Salimpour MR, Saber M, et al. Detailed analysis for the cooling performance enhancement of a heat source under a thick plate. *Energy Convers Manage* 2013;76:691–700.
- [2] Hajmohammadi MR, Moulod M, Shariatzadeh OJ, et al. Effects of a thick plate on the excess temperature of iso-heat flux heat sources cooled by laminar forced convection flow: conjugate analysis. *Numer Heat Transf Part A Appl* 2014;66(2):205–16.
- [3] Huebsch W, Munson B, Okiishi T, et al. *Fundamentals of fluid mechanics*; 2009.



Immunodetection of salivary biomarkers by an optical microfluidic biosensor with polyethylenimine-modified polythiophene-C₇₀ organic photodetectors



Tao Dong^{b,*,1}, Nuno Miguel Matos Pires^{a,1}

^a Institute of Applied Micro-Nano Science and Technology - IAMNST, Chongqing Key Laboratory of Colleges and Universities on Micro-Nano Systems Technology and Smart Transducing, Chongqing Engineering Laboratory for Detection, Control and Integrated System, National Research Base of Intelligent Manufacturing Service, Chongqing Technology and Business University, Nan'an District, Chongqing 400067, China

^b Department of Microsystems - IMS, Faculty of Technology, Natural Sciences and Maritime Sciences, University College of Southeast Norway, Postboks 235, 3603 Kongsberg, Norway

ARTICLE INFO

Keywords:

Immunosensor
Saliva diagnostics
Optical biosensor
Integrated microfluidics
Organic photodetector
Point-of-care

ABSTRACT

This work reports a novel optical microfluidic biosensor with highly sensitive organic photodetectors (OPDs) for absorbance-based detection of salivary protein biomarkers at the point of care. The compact and miniaturized biosensor has comprised OPDs made of polythiophene-C₇₀ bulk heterojunction for the photoactive layer; whilst a calcium-free cathode interfacial layer, made of linear polyethylenimine, was incorporated to the photodetectors to enhance the low cost. The OPDs realized onto a glass chip were aligned to antibody-functionalized chambers of a poly(methyl methacrylate) microfluidic chip, in where immunogold-silver assays were conducted. The biosensor has detected IL-8, IL-1 β and MMP-8 protein in spiked saliva with high detection specificity and short analysis time exhibiting detection limits between 80 pg mL⁻¹ and 120 pg mL⁻¹. The result for IL-8 was below the clinical established cut-off of 600 pg mL⁻¹, which revealed the potential of the biosensor to early detection of oral cancer. The detection limit was also comparable to other previously reported immunosensors performed with bulky instrumentation or using inorganic photodetectors. The optical detection sensitivity of the polythiophene-C₇₀ OPD was enhanced by optimizing the thickness of the photoactive layer and anode interfacial layer prior to the saliva immunoassays. Further, the biosensor was tested with unspiked human saliva samples, and the results of measuring IL-8 and IL-1 β were in statistical agreement with those provided by two commercial assays of ELISA. The optical microfluidic biosensor reported hereby offers an attractive and cost-effective tool to diagnostics or screening purposes at the point of care.

1. Introduction

Rapid, highly sensitive, and high-throughput detection of proteins is often a crucial step in clinical diagnostics and patient treatment. Certain diseases, such as cancer, cardiovascular diseases and (acute and chronic) systemic diseases, are related to small variations in the concentration of various proteins in body fluids (Joo et al., 2012; Rathnayake et al., 2013; Wei et al., 2009). Therefore, the early detection of disease-marker proteins using highly sensitive methods can save lives and minimize time-consuming and inexpensive treatments. Biomarker detection is commonly conducted by laboratory methods suffering from high costs and long analysis times. Consequently, there is increasingly clinical demand to develop novel inexpensive biosensors or point-of-care (POC) devices that can provide

more convenient test solutions (Cummins et al., 2016).

Among the body fluids tested in biosensors, saliva holds great promises in POC analysis (Nie et al., 2013; Thili et al., 2010), mainly due to the economic and non-invasive manner of sampling. The salivary fluid can be easily and painlessly collected by either patients or health care personnel and requires no use of needles, thus reducing the probability of blood-borne infections and enhancing patient compliance. Owing to the presence of various salivary biomarkers accurately reflecting the disease condition in humans, salivary diagnostics has shown clinical relevance in monitoring a wide range of diseases and health complications. For example, saliva carries a series of interleukins (e.g. IL-1 β and IL-8) and matrix metalloproteinases (e.g. MMP-8 and MMP-9) that can serve as biomarkers in a variety of human diseases including cancer, arthritis, cardiovascular disease and

* Corresponding author.

E-mail address: tao.dong@usn.no (T. Dong).

¹ The authors contributed equally and shared the first authorship.

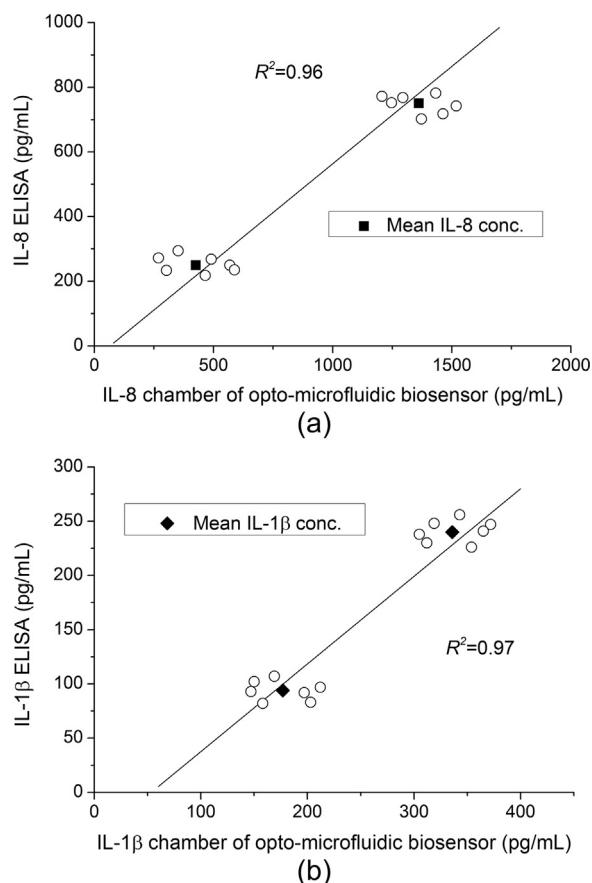


Fig. 5. Detection of human salivary IL-8 and IL-1 β using the optical microfluidic biosensor. The plots (a) and (b) show the measured results of two groups of IL-8 concentration and two groups of IL-1 β concentration, respectively, as detected by ELISA.

4. Conclusions

An optical microfluidic biosensor with polythiophene:PC₇₀BM BHJ OPDs for the detection of clinically relevant salivary biomarkers is described in this work. The biosensor has demonstrated good analytical performance for salivary IL-8, IL-1 β and MMP-8, exhibiting low detection limits, high detection specificity and reproducibility. The LOD for IL-8 was below the clinical established cut-off of 600 pg mL⁻¹, and was in same range as that of other previously reported immunosensors such as those utilizing electrochemical or fluorescence detection. The OPDs have incorporated a polymer cathode interlayer made of L-PEI compatible to solution-processable methods, which enhances the low cost of the organic photodetector and resultant biosensor.

The biosensor was further tested with human saliva samples, and the results were bench marked against two conventional absorbance assays of ELISA. Measurements of salivary biomarker concentrations were statistically correlated to those provided by ELISA. However, on contrary to ELISA performed with bulky optical instrumentation, the optical microfluidic biosensor can easily be realized in a portable and cost-effective device which makes it very attractive to POC settings. The proposed biosensor can also be extended to the detection of other protein biomarkers using other antibodies, thus finding application in diagnostics and screening of multiple diseases.

Acknowledgments

This work was supported by the National Natural Science Foundation of China (Grant nos. 61550110253 and 61650410655),

Regionale Forskningsfond Oslofjordfondet (Proj. nos. 234972, 249017, 258902 and 260586) and by Forprosjekt – VRIBEDRIFT Vestfold (Proj. no. 252173). The authors thank the support from Doctor Y. N. Xu at Chongqing Shuilun Hospital. The experimental studies were also supported by Out-patient Dept. at Chongqing Xiji Hospital and Henan University of Technology, School of Electrical Engineering. Our colleague Li Linbo is acknowledged for assistance and discussions on OPD fabrication processes. This research is also funded by Chongqing Research Program of Basic Research and Frontier Technology (Proj. nos. cstc2016jcyjA2161, cstc2015jcyjA20023), Science and Technology Research Program of Chongqing Education Commission (no. KJ1600604), and Chongqing Innovation Team of Colleges and Universities (no. CXTDX201601025).

Appendix A. Supporting information

Supplementary data associated with this article can be found in the online version at <http://doi:10.1016/j.bios.2017.03.005>.

References

- Ahn, C.-G., Ah, C.S., Kim, T.Y., Park, C.W., Yang, J.-H., Kim, A., Sung, G.Y., 2010. Appl. Phys. Lett. 97, 103703.
- Charwat, V., Purtscher, M., Tedde, S.F., Hayden, O., Ertl, P., 2013. Lab Chip 13, 785–797.
- Chen, H.-Y., Hou, J., Zhang, S., Liang, Y., Yang, G., Yang, Y., Yu, L., Wu, Y., Li, G., 2009. Nat. Photonics 3, 649–653.
- Chin, C.D., Linder, V., Sia, S.K., 2012. Lab Chip 12, 2118–2134.
- Cummins, B.M., Ligler, F.S., Walker, G.M., 2016. Biotechnol. Adv. 34, 161–176.
- Dong, T., Zhao, X., 2015. Anal. Chem. 87, 2410–2418.
- Honrado, C., Dong, T., 2014. J. Micromech. Microeng. 24, 125023.
- John, M.A.R.S., Li, Y., Zhou, X., Denny, P., Ho, C.-M., Montemagno, C., Shi, W., Qi, F., Wu, B., Sinha, U., Jordan, R., Wolinsky, L., Park, N.-H., Liu, H., Abemayor, E., Wong, D.T.W., 2004. Arch. Otolaryngol. Head Neck Surg. 130, 929–935.
- Joo, J., Kwon, D., Yim, C., Jeon, S., 2012. ACS Nano 6, 375–4381.
- Jóskowiak, A., Stasio, N., Chu, V., Prazeres, D.M.F., Conde, J.P., 2012. Biosens. Bioelectron. 36, 242–249.
- Kim, W.-J., Cho, H.Y., Kim, B.K., Huh, C., Chung, K.H., Ahn, C.-G., Kim, Y.J., Kim, A., 2015. Sens. Actuators B Chem. 221, 537–543.
- Liu, R., Liu, X., Tang, Y., Wu, L., Hou, X., Lv, Y., 2011. Anal. Chem. 83, 2330–2336.
- Lu, L., Xu, T., Chen, W., Landry, E.S., Yu, L., 2014. Nat. Photonics 8, 716–722.
- Nie, S., Benito-Peña, E., Zhang, H., Wu, Y., Walt, D.R., 2013. Anal. Chem. 85, 9272–9280.
- Pires, N.M.M., Dong, T., 2014. J. Biomed. Opt. 19 (3), 030504.
- Pires, N.M.M., Dong, T., Hanke, U., Hoivik, N., 2013. J. Biomed. Opt. 18, 097001.
- Pires, N.M.M., Dong, T., Hanke, U., Hoivik, N., 2014. Sensors 14, 15458–15479.
- Ploetz, E., Visser, B., Slingenberg, W., Evers, K., Martinez-Martinez, D., Pei, Y.T., Feringa, B.L., De Hosson, J.M., Cordes, T., van Dorp, W.F., 2014. J. Mater. Chem. B 2, 2606–2615.
- Qi, B., Zhang, Z.-G., Wang, J., 2015. Sci. Rep. 5, 7803.
- Rathnayake, N., Åkerman, S., Klinge, B., Lundegren, N., Jansson, H., Tryselius, Y., Sorsa, T., Gustafsson, A., 2013. PLoS One 8, e61356.
- Sia, S.K., Linder, V., Parviz, B.A., Siegel, A., Whitesides, G.M., 2004. Angew. Chem. Int. Ed. 43, 498–502.
- Tan, W., Sabet, L., Li, Y., Yu, T., Klokkevold, P.R., Wong, D.T., Ho, C.-M., 2008. Biosens. Bioelectron. 24, 266–271.
- Tlili, C., Cella, L.N., Myung, V.N., Shetty, V., Mulchandani, A., 2010. Analyst 135, 2637–2642.
- Torrente-Rodríguez, R.M., Campuzano, S., Montiel, V.R.-V., Gamella, M., Pingarrón, J.M., 2015. Biosens. Bioelectron. 77, 543–548.
- Williams, G., Backhouse, C., Aziz, H., 2014. Electronics 3, 43–75.
- Wei, F., Patel, P., Liao, W., Chaudhry, K., Zhang, L., Arellano-Garcia, M., Hu, S., Elashoff, D., Zhou, H., Shukla, S., Shah, F., Ho, C.M., Wong, D.T., 2009. Clin. Cancer Res. 15, 4446–4452.
- Wojciechowski, J.R., Shriver-Lake, L.C., Yamaguchi, M.Y., Fureder, E., Pieler, R., Schamesberger, M., Winder, C., Prall, H.J., Sonnleitner, M., Ligler, F.S., 2009. Anal. Chem. 81, 3455–3461.
- Wu, F.-C., Tung, K.-C., Chou, W.-Y., Tang, F.-C., Cheng, H.-L., 2016. Org. Electron. 29, 120–126.
- Yang, C.-Y., Brooks, E., Li, Y., Denny, P., Ho, C.-M., Qi, F., Shi, W., Wolinsky, L., Wu, B., Wong, D.T.W., Montemagno, C.D., 2005. Lab Chip 5, 1017–1023.
- Yang, Y., Chen, W., Dou, L., Chang, W.-H., Duan, H.-S., Bob, B., Li, G., Yang, Y., 2015. Nat. Photonics 9, 190–198.
- Yu, Z.T.F., Guan, H., Cheung, M.K., McHugh, W.M., Cornell, T.T., Shanley, T.P., Kurabayashi, K., Fu, J., 2015. Sci. Rep. 5 (11339).
- Zhang, L., Dong, T., 2013. J. Micromech. Microeng. 23, 045011.

A Compact Device for Urine Collection and Transport in Porous Media

Haakon Karlsen and Tao Dong^(✉)

University College of Southeast Norway, Borre, Norway
{Haakon.karlsen, tao.dong}@usn.no

Abstract. We investigate capillary flow in filter paper in compact point-of-care microfluidic devices for transport of liquid samples to sensing pads. Particular challenges were the effects of gravity, unintended capillaries, contamination and evaporation, and the purpose is to investigate solutions to achieve a robust device. On the condition that the liquid sample has sufficient time to saturate the filter paper, the transport of miscible liquid contaminants are mainly left to the mechanisms of diffusion, which was found to provide an inherent resistance to contamination. However, unintended capillaries between the filter paper and a surface provided an increase in the transport rate for both sample and contamination. This was avoided by sealing possible gaps on the sides of the filter paper with adhesive tape, and by applying a force perpendicular to the paper surface to flatten paper and prevent formation of air pockets between the filter paper surface and contacting surfaces.

Keywords: Biochemistry · Capillary flow · Point of care · Porous media

1 Introduction

Urinary tract infections (UTIs) are reported with high incidence for the elderly population [1], and is the highest for institutionalized or permanently hospitalized elderly [2]. UTIs can cause sepsis, and gram-negative sepsis are associated with a high mortality rate [3]. Many elderly in nursing homes suffer from urinary incontinence and often use adult diapers or other absorbent products [4]. Urinary incontinence can make voluntary collection of urine samples difficult, and catheterization as an alternative for urine sampling carries a risk of infection [5, 6].

Belmin et al. [7] showed high correlation between urine collected with catheter and extracted from diapers after 3 hours. However, urine residing for a long time in diapers increases the risk of contamination, which makes the sample less representative of the conditions in the bladder.

Paperbased fluidic devices are well suited for rapid diagnostic applications, and can be lightweight and disposable with low-cost fabrication. Paperbased fluidic devices can be driven by capillary flow in porous media, which does not require any external driving force [8]. For these reasons paperbased fluidic devices go well together with adult diapers.

5 Future Work

In the experiments, there were too much variance and too low time resolution in the initial stages to find a reasonably consistent estimate of a smooth knot point and the c parameter from Eq. 9 for segmented nonlinear regression. This was a preliminary investigation, and further work will improve the data collection in the beginning of the capillary flow.

Acknowledgement. Research supported by: Oslofjordfond projects, No: (1) 234972, (2) 249017, (3) 258902, (4) 255893. Research Council of Norway projects, No: (1) 251129, (2) 263783. National Natural Science Foundation of China, No: (1) 61531008, (2) 61550110253. Chongqing Research Program of Basic Research and Frontier Technology: No. cstc2015jcyjBX0004 Science and Technology Research Program of Chongqing Education Commission project, No: (1) KJ15006XX, (2) KJ1600602.

References

1. Nicolle, L.E.: Urinary tract infections in the elderly. *Clin. Geriatr. Med.* **25**(3), 423–436 (2009)
2. Hamilton-Miller, J.M.T.: Issues in urinary tract infections in the elderly. *World J. Urol.* **17**(6), 396–401 (1999)
3. Yoshikawa, T.T.: Unique aspects of urinary tract infection in the geriatric population. *Gerontology* **30**(5), 339–344 (1984)
4. Newman, D.K.: Incontinence products and devices for the elderly. *Urol. Nurs.* **24**(4), 316–333 (2004)
5. Nicolle, L.E.: Catheter-related urinary tract infection. *Drugs Aging* **22**(8), 627–639 (2005)
6. Warren, J.W.: Catheter-associated urinary tract infections. *Int. J. Antimicrob. Agents* **17**(4), 299–303 (2001)
7. Belmin, J., et al.: Reliability of sampling urine from disposable diapers in elderly incontinent women. *J. Am. Geriatr. Soc.* **41**(11), 1182–1186 (1993)
8. Yetisen, A.K., Akram, M.S., Lowe, C.R.: Paper-based microfluidic point-of-care diagnostic devices. *Lab Chip* **13**(12), 2210–2251 (2013)
9. De Gennes, P.-G., Brochard-Wyart, F., Quéré, D.: Hydrodynamics of interfaces: thin films, waves, and ripples. In: *Capillarity and Wetting Phenomena: Drops, Bubbles, Pearls, Waves*, pp. 107–138. Springer (2013)
10. Fries, N., Dreyer, M.: An analytic solution of capillary rise restrained by gravity. *J. Colloid Interface Sci.* **320**(1), 259–263 (2008)
11. Schwiebert, M.K., Leong, W.H.: Underfill flow as viscous flow between parallel plates driven by capillary action. *IEEE Trans. Compon. Packag. Manuf. Technol C* **19**(2), 133–137 (1996)
12. Choudhary, A., Kumar, D., Singh, J.: A fractional model of fluid flow through porous media with mean capillary pressure. *J. Assoc. Arab Univ. Basic Appl. Sci.* **21**, 59–63 (2016)

Zhongyuan Shi

From: Tao Dong <Tao.Dong@usn.no>
Sent: Sunday, May 28, 2017 6:39 PM
To: Zhongyuan Shi; Anh Tuấn Trần
Subject: Fwd: HEFAT2017 paper withdraw

From: Josua P Meyer <josua.meyer@up.ac.za>
Date: 28 May 2017 at 17:11:19 GMT+2
To: Tao Dong <tao.dong@usn.no>
Subject: HEFAT2017 paper withdraw

Dear Prof. Tao Dong

Manuscript number and title: #1570340431 'Geometric Optimization of Complex-Shaped Cavities According to Constructal Theory', for the HEFAT2016 conference.

1. The above paper was accepted for the HEFAT2017 conference.
2. The deadlines for registration and payment of the conference attendance fee were 21 May 2017.
3. It seems as if no author of the above paper linked this paper to their registration and/or paid the registration fee?
4. I have therefore changed the status of this paper to “withdraw”.
5. If this is incorrect then please inform me urgently within 72 hours.

Regards,
Prof Josua Meyer
CHAIR: HEFAT2017

GEOMETRIC OPTIMIZATION OF COMPLEX-SHAPED CAVITIES ACCORDING TO CONSTRUCTAL THEORY

Tuan Anh Tran¹ and Tao Dong^{1,*}

1. Department of Micro and Nano Systems Technology, Faculty of Technology, Natural Sciences and Maritime Sciences,
The University College of Southeast Norway (HSN),
Raveien 215, 3184 Borre, Bakkenteigen, Vestfold, Norway
Corresponding Author: anh tuan@dcselab.edu.vn, Tao.Dong@usn.no

ABSTRACT

Constructal principle is employed to optimize the configuration of a body that a complex shape of the cavity intruded into a solid conducting wall in this research. The main purpose is to minimize as much as possible the peak temperature and the distributed temperature gradient in the solid domain. The internal heat generation is assumed to be uniformly distributed throughout the solid wall. The cavity surface is isothermal, while the solid wall has adiabatic conditions on the outer surface. The total volume and the volume of the cavity are kept as constant, while the geometries of the cavity vary. This research represents clearly the investigation of several typical shapes of cavities including Fork shape, Phi and Psi shape, non-uniform X shape. Moreover, the comparison of heat transfer performance among these above-listed geometries is clearly discussed as well.

INTRODUCTION

Constructal theory has become much general in the current scientific society over the last decade. According to the Constructal law, a live system is one that has two universal characteristics: It flows and morphs freely toward configurations that allow all its currents to flow more easily over the time. Life and evolution are physics phenomenon, and they belong to physics.[1-3] The Constructal law is not a statement of optimization, maximization, minimization, or any other mental image of “end-design” or “destiny”. This is about the direction of evolution in time, and the fact that the design phenomenon is not certain: It is dynamic, ever changing. Hence, evolution never ends.

There is such a principle, and it is based on the universal observation that if a flow system is endowed with sufficient freedom to change its configuration, the system exhibits configurations that provide progressively better access routes for the currents that flow. The Constructal field started from the realization that “design” is a universal physics phenomenon. It unites the animate with the inanimate over an extremely broad range of scales, from the tree-shaped design of the snowflake, to animal design.[4]

The optimal structure is constructed by optimizing volume shape at every length scale, in a hierarchical sequence that begins with the smallest building block, and proceeds towards larger building blocks. The concepts of life, design, and future (evolution) were placed certainly in physics as follows: “For a finite-size system to persist in time (to live), it must evolve in such a way that it provides easier access to the imposed (global) currents that flow through it.”[1]

In practical domain, miniaturization and density integration have been recently the state-of-the-art technologies. After remarkable technological progress, the technology of electronic cooling has been made on pushing the frontier and continuing works have been conducted in the related areas. Although individual solid-state electronic devices are inherently reliable, a single microelectronic chip may contain various components and thus, obtaining failure-free operation over the useful life of a product is a violently challenging. In this technology, the biggest challenge is to maintain the maximum temperatures of the heat generating body below an allowable level [1], owing that the performance of equipment has a direct relationship with its temperature. As a result, many opinions have been proposed to enhance the cooling efficiency of electronic components with high heat flux generation and compact size. Consequently, convective channels and conductive routes have attracted more attentions. Recognition of conduction pathways also take up space, effective conduction routes need to be designed to be well-suited for the miniaturization evolution.[2]

Fortunately, Bejan has clarified toward the ‘volume-to-point’ flow problems. He considered a finite-size volume in which heat is generated at every point and which is cooled through a heat sink in the rim. The goal was to minimize the maximum temperature by determining the optimal distribution of

high conductivity material when a limited amount of high conductivity material is available. On the basis of constructal law of design and evolution [2-4], he indicated the solution to this problem is a ‘tree shape’, with far reaching implications in physics, mathematics and the natural evolution of living systems.

Apart from this valuable achievement, other research works were also defined relying on the basis of his studies. For instance, Lorente and Bejan [5] proposed a non-uniformly distribution of high conductive material and achieved a remarkable improvement in the global performance. Optimal configurations of highly conductive materials at micro and nano-scales were also determined. Discrete variable cross-section conducting paths of inserts were also defined. Most recently, numerical studies have been figured out on the optimization of conductive inserts. It introduced uniform and non-uniform X-shaped pathways of higher thermal conductivity and illustrated that the studied shape is superior in minimizing the maximum temperature [3].

As a result, it is given that the competition for the achievement of “ideal” structure of highly conductive pathways still grows up. Cavities are defined as the regions formed between adjacent fins and stand for the essential promoters of nucleate boiling or condensation. In this sense, creative types of conductive pathways containing “Phi-Psi” shape or advantaged fork shape are introduced. Although these pathways are in the similar class as the “tree-shaped” configuration discovered in the very first paper [1], it is illustrated that the bend sections that are placed in ‘Phi’ and ‘Psi’ shaped inserts improve the tree-shaped configurations (also X, T, H and I-shaped configurations).

Obviously, the optimal procedure of several cavities contains various levels in order to figure out how variables vary to obtain the peak temperature and smallest temperature gradient within the solid body. Furthermore, the comparison of heat transfer efficiency (similar volume ratio) among these designed shapes in conclusively summarized in this paper as well.

NOMENCLATURE

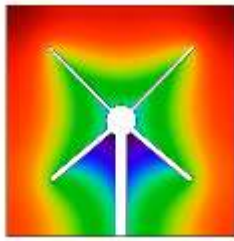
A	[m ²]	Area
D	[m]	Length
H	[m]	Height
k	[W/mK]	Thermal conductivity
\dot{Q}	[W/m ³]	Uniform volumetric heat generation in the cavities
R	[m]	Radius
T	[K]	Local temperature
x, y, z	[m]	Cartesian axis direction
V	[m ³]	Volume
W	[m]	Width
Greeks symbols		
ω	[-]	Volume fraction occupied by the insert
λ	[-]	Thermal conductivity ratio, k_b/k_i
α	[rad]	Angle between the inferior branch of the X and the x axis
β	[rad]	Angle between the superior branch of the X and the x axis
θ	[-]	Dimensionless temperature
ϕ	[-]	Area fraction
Subscripts		
b		Base shaped part of the insert
h		High conductivity materials (insert)
i		Inner ring
l		Low conductivity materials (heat generating piece)
m		Minimized
max		Maximum
min		Minimum
o		Optimized/outer ring
r		ring shaped part of the insert
s		Stem shaped part of the insert

C. Non-uniform X insert

In order to understand the effect of each degree of freedom on the geometry configuration and thermal performance, the investigation of the optimal shape is performed in two steps. In the first step, we start by simulating the effect of the β angle. Figure 15 shows that there is an optimal β angle that minimizes the dimensionless maximal excess of temperature for several values of α angle when the degrees of freedom L_1/L_0 , L_2/L_0 , D_1/D_0 , D_2/D_0 , and ϕ area fraction are fixed.

For instance, for $\alpha = 0$ rad, θ_{\max} decreases until $b_0 = 0.47$ and after this value θ_{\max} shows only a slight increase. On the opposite, for $\alpha = -0.7$ rad, it is observed a significant decrease of θ_{\max} until the minimal value and, after this point, it is noticed a step increase of θ_{\max} . This figure also indicates that there is a second opportunity of optimization (the second step).

a)



b)

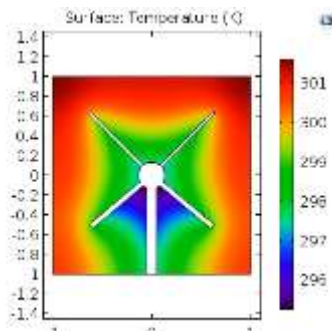


Figure 14ab Non-uniform X-shaped design

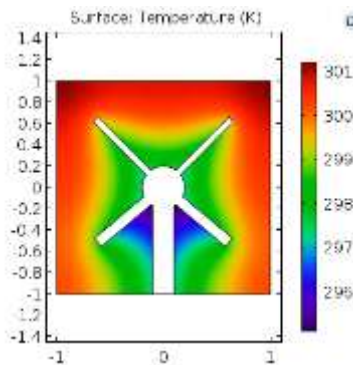


Figure 15 Optimal Non-uniform X-shaped geometry

Therefore, the minimal dimensionless maximal excess of temperatures θ_{\max} , calculated as a function of β -angle. This figure shows that the twice minimized $\theta_{\max} = 0.03956$ is obtained when the optimal angle α is $\alpha_0 = -0.7$.

CONCLUSION

In this present research, we conducted a study involving several types of tree-shaped conductive inserts. Particularly, we have been figuring out the detailed optimization process to obtain the best geometries of above-mentioned insert. Thus, we meet up the main purpose of minimizing the peak temperature and the temperature gradient distributed within the square body. We discovered that, compared with the existing configurations mentioned in literature, the heat generating body operates at the lower level of peak temperature depending on

the volume fraction of the inserts and the thermal conductivity ratio. Also, the Psi-shaped configuration is found superior to the Phi-shaped insert.

Typically, when the objective is at a minimization of the peak temperature, it is shown that the maximum temperature obtained by Psi inserts can be reduced by 50% or higher compared to the X-shaped pathways. Otherwise, the minimum temperature achieved in Phi-shaped case is about 20% lower than that in the X-shaped one. Furthermore, it is addressed that the maximum temperature can be reduced by 41% by using "F1" inserts compared with the X-shaped pathways. The superiority of fork-shaped insert over the X-shaped one is found about 46% in the case of "F2" inserts. Additionally, the cooling efficiency by applying T, Y and H inserts is considered approximately similar for each other. An advanced T-Y insert is constructed to present advantages in heat transfer domain.

However, due to the concerns associated with the cost efficiency and space of high conductivity materials, the foregoing achievement and the advance achieved in the future are very necessary for scientists to engage with the empirical design of highly conductive pathways. We also mentioned that if only one third amount of high conductivity materials used for an X-shaped insert are used in a Psi-shaped insert, the heat generating body operate at the same level of peak temperature. Hopefully, we expect further in-depth investigations from advanced research groups all over the world in the near future.

ACKNOWLEDGEMENTS

Master student Tuan Anh Tran is sincerely thankful Dr. Zhongyuan Shi for his advice in order to complete this research. The present work is originated from the final project report for the course MN-HMT5900 at HSN. The financial support from Chongqing Research Program of Basic Research and Frontier Technology (No. cstc2015jcyjBX0004), Science and Technology Research Program of Chongqing Education Commission (No. KJ1600602 & No. KJ15006XX), Forskningsrådet Nærings-Ph.D. (Project No.: 251129), Regionale Forskningsfond Oslofjordfondet (Project No.: 258902) and NANO2021 (Project No.: 263783) is hereby acknowledged. This paper is also going to be published in 13th International Conference on Heat Transfer, Fluid Mechanics and Thermodynamics (HEFAT) held in Slovenia in July 2017.

REFERENCES

- [1] Bejan, A., 2000, Shape and Structure, *From Engineering to Nature*, Cambridge University Press, Cambridge, UK.
- [2] Bejan, A., 1997, *Advanced Engineering Thermodynamics*, 2nd ed., Wiley, New York, Chap. 13.
- [3] Bejan, A., 1997, "Constructal-Theory Network of Conducting Paths for Cooling a Heat Generating Volume," *Int. J. Heat Mass Transfer*, 40, pp. 799–816.
- [4] Bejan, A., 1997, "Theory of Organization in Nature: Pulsating Physiological Processes," *Int. J. Heat Mass Transfer*, 40, pp. 2097–2104.
- [5] Bejan, A., and Lorente, S., 2004, "The Constructal Law and the Thermodynamics of Flow Systems With Configuration," *Int. J. Heat Mass Transfer*, 47, pp. 3203–3214.
- [6] A. Bejan, G.W. Merx, *Constructal Theory of Social Dynamics*, Springer, New York, 2007.
- [7] N. Dan, A. Bejan, Constructal tree networks for the time-dependent discharge of finite-size volume to one point, *J. Appl. Phys.* 84 (6) (1998) 3042-3050.
- [8] M. Almgöbel, A. Bejan, Conduction trees with spacings at the tips, *Int. J. Heat Mass Transfer*, 42 (20) (1999) 3739-3756.
- [9] S. Lorente, W. Wechsattel, A. Bejan, Optimization of tree-shaped flow distribution structures over a disc-shaped area, *Int. J. Energy Res.* 27 (8) (2003) 715-723.
- [10] W. Wu, L. Chen, F. Sun, On the "area to point" flow problem based on constructal theory, *Energy Convers. Manage.* 48 (1) (2007) 101-105.
- [11] L. Chen, S. Wei, F. Sun, Constructal entransy dissipation minimization for volume-point heat conduction, *J. Phys. D: Appl. Phys.* 41 (19) (2008) 195506.
- [12] A. Bejan, M.R. Errera, Convective trees of fluid channels for volumetric cooling, *Int. J. Heat Mass Transfer*, 43 (17) (2000) 3105-3118.
- [13] A. Bejan, L.A.O. Rocha, S. Lorente, Thermodynamic optimization of geometry: T and Y-shaped constructs of fluid streams, *Int. J. Thermal Sci.* (39) (2002) 949-960.
- [14] A.H. Reis, A.F. Miguel, A. Bejan, Constructal theory of particle agglomeration and design of air-cleaning devices, *J. Phys. D: Appl. Phys.* 39 (10) (2006) 2311-2318.
- [15] W. Wechsattel, S. Lorente, A. Bejan, Tree-shaped insulated designs for the uniform distribution of hot water over an area, *Int. J. Heat Mass Transfer*, 44 (16) (2001) 3111-3123.
- [16] C. Biserni, L.A.O. Rocha, G. Stanesco, E. Lorenzini, Constructal H-shaped cavities according to Bejan's theory, *Int. J. Heat Mass Transfer*, 50 (11-12) (2007) 2132-2138.
- [17] C. Biserni, L.A.O. Rocha, A. Bejan, Inverted fins: geometric optimization of the intrusion into a conducting wall, *Int. J. Heat Mass Transfer*, 47 (12-13) (2004) 2577-2583.
- [18] M. Almgöbel, A. Bejan, Conduction trees with spacings at the tips, *Int. J. Heat Mass Transfer*, 42 (20) (1999) 3739-3756.
- [19] G. Lorenzini, C. Biserni, L.A.O. Rocha, Constructal design of X-shaped conductive pathways for cooling a heat-generating body, *Int. J. Heat Mass Transfer*, 58 (2013) 513-520.

Zhongyuan Shi

From: EDAS Conference Manager <help@edas-help.com> on behalf of HEFAT2017 <hefat2017-chairs@edas.info>
Sent: Monday, May 1, 2017 4:36 PM
To: Per Kristian Bolstad; Zhongyuan Shi; Tao Dong
Subject: [HEFAT2017] Your paper #1570340714 ('Constructal Design of Cavities for Intensified Cooling Performance on Heat Generating Volumes')

Dear Mr. Per Kristian Bolstad:

Congratulations - your paper #1570340714 ('Constructal Design of Cavities for Intensified Cooling Performance on Heat Generating Volumes') for HEFAT2017 has been accepted, and will be scheduled in the track Poster Presentations.

Please register for the conference; using the registration icon after logging in on: <http://edas.info/>

Also as soon as possible pay your registration fee and accommodation. The accommodation is limited and it is crucial that you finalize it as soon as possible. You may also directly download your official acceptance letter and/or letter require for a visa application by clicking on the “visa icon”.

Regards, Josua Meyer
CHAIR: HEFAT2017

CONSTRUCTAL DESIGN OF CAVITIES FOR INTENSIFIED COOLING PERFORMANCE ON HEAT GENERATING VOLUMES

Per Kristian Bolstad¹, Zhongyuan Shi^{2,3,4}, Tao Dong^{1,*}

1. Department of Microsystems, Faculty of Technology, Natural Sciences and Maritime Sciences, University College of Southeast Norway (HSN), 3184 Borre, Norway
2. Institute of Applied Micro-Nano Science and Technology, Chongqing Key Laboratory of Colleges and Universities on Micro-Nano Systems Technology and Smart Transduction, National Research Base of Intelligent Manufacturing Service, Chongqing Technology and Business University, 19 Xuefu Ave., Nan'an District, Chongqing, China
3. Chongqing Engineering Laboratory for Detection, Control and Integrated System, Chongqing Technology and Business University, 19 Xuefu Ave., Nan'an District, Chongqing, China
4. Department of Mathematics, Faculty of Mathematics and Natural Sciences, University of Oslo, P.O. box 1053, Blindern, 0316 Oslo, Norway

* Corresponding Author: tao.dong@usn.no

ABSTRACT

The study of heat conduction in micro systems is a topic of interest as heat generation is a common issue in electronics. This paper will study heat conduction, using finite element simulations of a cross-sectional copper surface with micro channels where the thermal conductivity of the coolant fluid is set to 0.591 W/(m·K), which corresponds to water at 293 K. The simulated models are made using COMSOL Multiphysics 5.2a. Heat Transfer module allows for the study of heat transfer in devices. The bottom and side surfaces of the heat sink are thermally isolated. The top surface is assigned a general inward heat flux of 10 MW/m². The channel structure is designed following the Allometric law. For a Y-design, 45° angles are used between one bifurcation level and the next, and 90° for the T-design. A steady state situation is defined, and a laminar flow at constant temperature is designated for the fluid in the channels. Looking at this as a fully developed region with constant surface temperature, the Nusselt number can be considered constant. The heat transfer coefficient assigned to the channels is obtained from calculations related to the channel dimensions and the previously mentioned boundary conditions. The respective Darcy friction factor, pressure drop and nominal pumping power is calculated for each of the designs. The resulting simulations show the diffusion dominated heat conduction of the heated area. The Y-design is shown to be the superior design for heat conduction.

INTRODUCTION

Heat fluxes in different materials and products are important issues to solve, hence the construction of electronic devices being smaller and closer packaged creates a need for micro cooling systems. Air-cooling systems have a limit of 100W/cm². By using cooling liquids and systems consisting of micro channels, it should be possible to deliver a heat dissipation rate closer to 1kW/cm², (10MW/m²) with a junction-to-air temperature difference of 50°C [1].

In nature, the tree shape is often found in different variations, such as veins in the body, river basins and roots and branches of trees. The branching networks consists of a main branch which bifurcates into thinner and shorter branches, and this is repeated n times. The structure is based on the constructal law which gives the most efficient transport of fluids and heat due to the hydrodynamics in such a system [2]. The constructional law first formulated by Adrian Bejan in 1996, states: "For a flow to persist in time (to survive), it must evolve in such a way that it provides easier and easier access to the currents that flow through it". According to this theory, if a flow system has sufficient freedom to change its configuration, pattern and geometry, then the system will progressively improve access routes for the currents that flow within that system over time [7].

Experiments are done using a tree structure with rectangular channels comparing this to parallel channels, arguing that this gives place to an increase of convective heat transfer and that it reduces the pressure drop [3].

Using branched network of micro channels embedded in a heat generating volume connected to a heat sink, shows that more complex structures increase the cooling performance, but also that there are limitations, which result in some designs being more optimal [4] [5].

Further experiments comparing Y-shaped and Ψ-shaped structures with various number of bifurcation levels, concludes that Ψ-shaped structures have better heat transfer characteristics such as lower thermal resistance and higher surface temperature uniformity. This is mainly caused due to a more uniform distribution of the channels [6].

This information is used as a base for considering how to design the structures desired for this project.

NOMENCLATURE

Nu_D	[-]	Nusselt number
h	[W/m ² K]	Heat transfer coefficient

Figure 6 shows the temperature distribution of the block in Kelvin. The colors indicate the thermal gradient moving from warm at the top surface to colder towards the bottom. The areas around the first, second and third branch are effectively cooled. The heat from the top surface is drawn towards the opening of the “Y-shape”. The average surface temperature using this channel design is 295.74 K.

By comparing Figure 5 and Figure 6, it is clear that the “Y-shape” surpasses the “T-shape” in terms of cooling the block both more efficiently and evenly. The design dimensions of the block and channels, as well as the temperature range, is the same for both figures. The average temperature of Figure 6 is lower than that of Figure 5, indicating a better cooling performance.

One of the reasons the Y-shaped design is more efficient than the T-shaped design is the more conveniently distributed channels over the cross-sectional area of the heat sink. The “T-shaped channel” design is proven less effective due to a more compact area covered by cooling channels. By opening the ramifications at 45° angles is more effective than 90° angles. It is also a possibility that the bifurcation angle may have some effect on the heat transfer inside the channels, but this was not considered in this project.

CONCLUSION

For an inward heat flux of 10 MW/m², the “Y-shape” design conducts the heat more efficiently. This design gives a lower average surface temperature, which is clearly beneficial. It can therefore be concluded that the “Y-shape” design is the superior design. It is also clear that the distance between the parallel channels is an important factor to create an effective design, where the thinner channels remove heat at a higher rate than thicker channels, at least in the order of dimensions used in this project.

The pressure drop in the thinner channels are higher than that of the thicker channels, thus a higher pumping power is required to maintain steady flow.

The simulations presented in this paper will be followed up by experimental research. The future work will be to test the channel systems in a realistic case where the flows in the channel are taken into account. This can be done by fabricating the designed models and building a pumping circuit for the channels.

ACKNOWLEDGMENTS

The present work is originated from the final report for the course MN-HMT5900 at HSN. Mette Vægg has made a great contribution to the original report. The financial support from Chongqing Research Program of Basic Research and Frontier Technology (No. cstc2015jcyjBX0004), Science and Technology Research Program of Chongqing Education Commission (No. KJ1600602 & No. KJ15006XX), Forskningsradet Nærings-Ph.D. (Project No.: 251129), Regionale Forskningsfond Oslofjordfondet (Project No.: 258902) and NANO2021 (Project No.: 263783) is hereby acknowledged.

REFERENCES

- [1] S. G. Kandlikar, “High flux heat removal with microchannels - A roadmap of challenges and opportunities,” *Heat Transfer Engineering*, vol. 26, no. 8, pp. 5–14, 2005.
- [2] A. Bejan and S. Lorente, “*Design With Constructal Theory*,” ResearchGate, vol. 22, no. 1, Jan. 2006.
- [3] Y. Chen and P. Cheng, “An experimental investigation on the thermal efficiency of fractal tree-like microchannel nets,” *ResearchGate*, vol. 32, no. 7, pp. 931–938, Jul. 2005.
- [4] X.-Q. Wang, A. S. Mujumdar, and C. Yap, “Numerical Analysis of Blockage and Optimization of Heat Transfer Performance of Fractal-like Microchannel Nets,” *J. Electron. Packag.*, vol. 128, no. 1, pp. 38–45, May 2005.
- [5] X.-Q. Wang, A. S. Mujumdar, and C. Yap, “Effect of bifurcation angle in tree-shaped microchannel networks,” *Journal of Applied Physics*, vol. 102, no. 7, p. 73530, Oct. 2007.
- [6] C. A. Rubio-Jimenez, A. Hernandez-Guerrero, J. G. Cervantes, D. Lorenzini-Gutierrez, and C. U. Gonzalez-Valle, “CFD study of constructal microchannel networks for liquid-cooling of electronic devices,” *Applied Thermal Engineering*, vol. 95, pp. 374–381, Feb. 2016.
- [7] A. Bejan, “Constructal theory of pattern formation,” *Hydrology and Earth System Sciences Discussions*, vol. 11, no. 2, pp. 753–768, Jan. 2007.
- [8] “Thermal conduction,” *Wikipedia*. 21-Nov-2016.
- [9] “Convection,” *Wikipedia*. 14-Dec-2016.
- [10] “Basic Microfluidic Concepts.” [Online]. Available: <http://faculty.washington.edu/yagerp/microfluidicstutorial/basicconcepts/basicconcepts.htm>. [Accessed: 20-Dec-2016].
- [11] C. Nonino, S. Savino, S. Del Giudice, and L. Mansutti, “Conjugate forced convection and heat conduction in circular microchannels,” *International Journal of Heat and Fluid Flow*, vol. 30, no. 5, pp. 823–830, Oct. 2009.
- [12] H. A. Mohammed, G. Bhaskaran, N. H. Shuaib, and R. Saidur, “Heat transfer and fluid flow characteristics in microchannels heat exchanger using nanofluids: A review,” *ResearchGate*, vol. 15, no. 3, pp. 1502–1512, Apr. 2011.
- [13] “The Nusselt Number.” [Online]. Available: <http://pages.jh.edu/~virtlab/heat/nusselt/nusselt.htm>. [Accessed: 21-Dec-2016].
- [14] COMSOL Multiphysics version 5.2a. Stockholm, Sweden. COMSOL, 2016.
- [15] “Thermal Conductivity of some common Materials and Gases.” [Online]. Available: http://www.engineeringtoolbox.com/thermal-conductivity-d_429.html. [Accessed: 21-Dec-2016].
- [16] Y. S. Touloukian, P. E. Liley, and S. C. Saxena, “Thermophysical Properties of Matter - The TPRC Data Series. Volume 3. Thermal Conductivity - Nonmetallic Liquids and Gases,” Jan. 1970.
- [17] A. Bejan and A. D. Kraus, *Heat Transfer Handbook*. John Wiley & Sons, 2003.
- [18] Matlab version R2016b. Natick, MA, U.S.A., The MathWorks Inc., 2016.



(12)发明专利申请

(10)申请公布号 CN 106610316 A

(43)申请公布日 2017. 05. 03

(21)申请号 201611246082.3

(22)申请日 2016.12.29

(71)申请人 重庆工商大学

地址 400067 重庆市南岸区学府大道19号
重庆工商大学

申请人 挪威三色帆有限公司
挪威三叶虫微系统有限公司

(72)发明人 董涛 史中远 杨朝初
埃里克·本特森·埃格兰

(74)专利代理机构 重庆百润洪知识产权代理有
限公司 50219

代理人 高姜

(51) Int. Cl.

G01J 5/00(2006.01)

权利要求书2页 说明书6页 附图2页

(54)发明名称

基于热波动耦合红外成像的薄壁局部换热系数测量方法

(57)摘要

本发明公开了基于热波动耦合红外成像的薄壁局部换热系数测量方法,利用一维非稳态导热方程在一侧(参考侧,换热系数已知)为周期性热流边界条件下的解析解,获得与参考侧壁温和所施加热流波动信号之间的相位差存在单值函数关系的薄壁另一侧(待测侧)的稳态局部换热系数。本技术方案不受红外热成像仪测温精度的影响,可通过对参考侧的热扰动和基于红外成像的薄壁表面温度信号采集实现非接触式薄壁特征表面局部换热系数的快速测量。

